

Long quantum channels for high-quality entanglement transfer

L. Banchi,^{1,2} T. J. G. Apollaro,¹ A. Cuccoli,^{1,2} R. Vaia,³ and P. Verrucchi^{3,1,2}

¹*Dipartimento di Fisica, Università di Firenze, Via G. Sansone 1, I-50019 Sesto Fiorentino (FI), Italy*

²*INFN Sezione di Firenze, via G.Sansone 1, I-50019 Sesto Fiorentino (FI), Italy*

³*Istituto dei Sistemi Complessi, Consiglio Nazionale delle Ricerche,
via Madonna del Piano 10, I-50019 Sesto Fiorentino (FI), Italy*

(Dated: November 26, 2024)

High-quality quantum-state and entanglement transfer can be achieved in an unmodulated spin bus operating in the ballistic regime, which occurs when the endpoint qubits A and B are coupled to the chain by an exchange interaction j_0 comparable with the intrachain exchange. Indeed, the transition amplitude characterizing the transfer quality exhibits a maximum for a finite optimal value $j_0^{\text{opt}}(N)$, where N is the channel length. We show that $j_0^{\text{opt}}(N)$ scales as $N^{-1/6}$ for large N and that it ensures a high-quality entanglement transfer even in the limit of arbitrarily long channels, almost independently of the channel initialization. For instance, the average quantum-state transmission fidelity exceeds 90 % for any chain length. We emphasize that, taking the reverse point of view, should j_0 be experimentally constrained, high-quality transfer can still be obtained by adjusting the channel length to its optimal value.

I. INTRODUCTION

Quantum state transfer between distant qubits (say, A and B) is a fundamental tool for processing quantum information. The task of covering relatively large distances between the elements of a quantum computer, much larger than the qubit interaction range, can be achieved by means of a suitable communication channel connecting the qubits A and B.

Spin chains are among the most studied channel prototypes [1]. In particular, the XY $S=1/2$ model has been widely employed as a tool for testing and analyzing quantum communication protocols. For such a communication channel to be experimentally feasible one could be lead to consider systems with uniform intrachannel interactions [2–8] and whose operation does not require peculiar initialization procedures, although other proposals have been recently put forward [9–12]. On the other hand, the quantum-transfer capabilities of homogeneous spin channels have not yet been fully explored under many respects. For instance, it is a common belief that the longer the chain the worse is the transmission fidelity [1, 2, 13, 14] as an effect of dispersion, and chains up to only a few tenths of spins are often considered.

The present work is devoted to the study of the ballistic regime, where the transmission can be depicted [6, 15, 16] in terms of a traveling wavepacket carrying the information about the state of the endpoint qubit A, eventually yielding the state reconstruction at the opposite endpoint qubit B thanks to the overall system's mirror symmetry [9–11, 17]. The ballistic regime differs from that arising in the limit of very weak endpoint couplings [3, 5, 18, 19] where (almost) perfect state transfer occurs at very long times as a result of a Rabi-like population transfer involving only the lowest-energy single-particle modes. Understanding the basic mechanism of ballistic transfer, where the number of involved single-particle modes will be shown to be of the order of $N^{2/3}$, allows us to devise an optimal value of the endpoint in-

teractions for any N , and vice versa. Remarkably, the corresponding transmission quality, as witnessed by the state- and the entanglement fidelity, does not decrease to zero when the channel becomes very long, but remains surprisingly high.

We consider the setup illustrated in Fig. 1: the channel connecting the qubits A and B is a one-dimensional array of N localized $S = 1/2$ spins with exchange interactions of XX Heisenberg type and a possible external magnetic field applied along the z direction. This gives the total Hamiltonian the following structure

$$\mathcal{H} = - \sum_{i=1}^{N-1} (S_i^x S_{i+1}^x + S_i^y S_{i+1}^y) - h \sum_{i=1}^N S_i^z \quad (1)$$
$$- j_0 \sum_{i=0, N} (S_i^x S_{i+1}^x + S_i^y S_{i+1}^y) - h_0 (S_0^z + S_{N+1}^z),$$

where the qubits A and B sit at the endpoint sites 0 and $N+1$ of a one-dimensional discrete lattice on whose sites $1, 2, \dots, N$ the spin chain is set. The exchange interaction (chosen as energy unit) and the magnetic field h are homogeneous along the chain, and an overall mirror symmetry is assumed, implying the endpoint coupling j_0 and field h_0 to be the same for both ends. The N spins constituting the XX channel are collectively indicated by Γ . We will focus our attention on how the state of the qubit B evolves under the influence of the chain Γ , and depending on the initial state of the qubit A; the latter is possibly entangled with an ancillary qubit C. The results of the analysis are used for gathering insights on the quantum-information transmission through the chain, so as to characterize the dynamical evolution of the overall system and to maximize the quality of the quantum-state transfer.

Even though the overall scheme could also be used for realizing tasks other than quantum information transfer, via the dynamical correlations that the chain induces between A and B [20], our approach is specifically tailored for studying transfer processes along the chain: the qubit

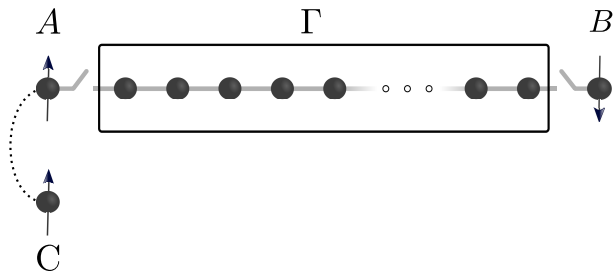


FIG. 1. The endpoints of a quantum channel Γ are coupled to the qubits A and B, via a tunable interaction j_0 ; A can be entangled with an external qubit C.

B or the qubit-pair BC are considered as target system, depending on whether the quantum-state of the qubit A or that of the qubit-pair AC are to be transferred, respectively.

In Section II the formalism used to study the dynamical evolution of the composite system is introduced and we derive the corresponding time-dependent expressions for the quantities used for estimating the quality of the quantum-state and entanglement transfer processes. In Section III the proposed formalism is applied to the XX model described by Eq. (1). In Section IV we put forward an analytical framework in order to improve the understanding of the conditions inducing an optimal ballistic dynamics. The resulting high-quality transfer processes along the spin chain are analyzed in Section V. Conclusions are drawn in Section VI, where comments about possible implementation of the procedure are also put forward. Relevant details of calculations are reported in the Appendices.

II. DYNAMICS AND TRANSFER QUALITY

A. Dynamics

The density matrix of a qubit B can be written as $\rho = \sum_{\mu} b_{\mu} \zeta_{\mu}$ where $\mu = 1, \dots, 4$, b_{μ} are complex numbers, and $\{\zeta_{\mu}\}$ is an orthonormal basis in the Hilbert space of 2×2 matrices endowed with the Hilbert-Schmidt trace-product, $\text{Tr}[\zeta_{\mu}^{\dagger} \zeta_{\nu}] = \delta_{\mu\nu}$. In some cases it is useful to choose Hermitian ζ_{μ} , for instance the identity and the three Pauli matrices. However, a more direct connection with the computational basis $\{|0\rangle \equiv |\uparrow\rangle, |1\rangle \equiv |\downarrow\rangle\}$ for the pure states of B is established by choosing $\zeta_{\mu} = |i\rangle\langle j|$ and setting $\mu = 1 + 2i + j$, with $i, j = 0, 1$. In what follows we will use this description, and hence use indices μ, ν, λ running from 1 to 4, understanding summation over any repeated index, e.g., $\rho = b_{\mu} \zeta_{\mu}$. Hermiticity of ρ implies b_1 and b_4 to be real and $b_2 = b_3^*$, while $\text{Tr} \rho = 1$ means $b_1 + b_4 = 1$, so that only three real parameters are independent. The positivity of ρ requires that $|b_2|^2 \leq b_1 b_4$.

The dynamics of B is described by its time-dependent

density operator $\rho(t)$; this can always be expressed as a linear function of a suitable input density matrix ρ^{in} , which may be the initial one of qubit B itself or that of any other qubit playing a role in its evolution:

$$\rho(t) = \mathcal{E}_t \rho^{\text{in}}, \quad (2)$$

where the quantum operation \mathcal{E}_t is a trace-preserving, completely positive, convex-linear map from *input* density operators ρ^{in} to density operators of the qubit at time t (see, e.g., Ref. 21). The effect of the linear map can be represented in terms of a 4×4 time-dependent matrix

$$T_{\mu\nu}(t) = \text{Tr} [\zeta_{\mu}^{\dagger} \mathcal{E}_t \zeta_{\nu}]. \quad (3)$$

In fact, by writing $\rho(t) = b_{\mu}(t) \zeta_{\mu}$ and $\rho^{\text{in}} = a_{\nu} \zeta_{\nu}$, one gets

$$b_{\mu}(t) = T_{\mu\nu}(t) a_{\nu}. \quad (4)$$

If B is part of a larger system S ruled by a total Hamiltonian \mathcal{H} and prepared in the initial state ρ^{tot} , it is also

$$b_{\mu}(t) = \langle \zeta_{\mu}^{\dagger}(t) \rangle, \quad (5)$$

where $\langle \cdot \rangle \equiv \text{Tr}[\cdot \rho^{\text{tot}}]$ and $\zeta_{\mu}(t) = e^{i\mathcal{H}t} \mathbb{1}_{S \setminus B} \otimes \zeta_{\mu} e^{-i\mathcal{H}t}$, ζ_{μ} acting on the Hilbert space of the qubit B. The matrix elements $T_{\mu\nu}(t)$ explicitly follow from Eq. (4) and (5).

Here we will essentially focus on the time evolution of the qubit B and take the input density operator in Eq. (2) to represent the initial state of the qubit A, as this is the most natural setup for studying quantum state and entanglement transmission processes from A to B. Referring to the specific setup described in Fig. 1 we prepare the overall system $A \cup \Gamma \cup B$ in the initial state $\rho^{\text{tot}} = \rho^A \otimes \rho^{\Gamma} \otimes \rho^B$ and let it evolve into $e^{-i\mathcal{H}t} \rho^{\text{tot}} e^{i\mathcal{H}t}$, where \mathcal{H} is the total Hamiltonian (1). Notice that ρ^{tot} has a fully separable structure: this is not a necessary condition for the explicit determination of the dynamical matrix (a structure such as $\rho^A \otimes \rho^{\Gamma B}$ would also work), but it is quite meaningful in our scheme, as the qubit B is assumed not to interact with the chain during the initialization process, which makes quite artificial its being entangled with the chain before the dynamics starts.

The density matrix of B evolves according to $\rho^B(t) = \text{Tr}_{A \cup \Gamma} [e^{-i\mathcal{H}t} \rho^{\text{tot}} e^{i\mathcal{H}t}]$, from which

$$\begin{aligned} T_{\mu\nu}(t) &= \text{Tr}_B \left[\zeta_{\mu}^{\dagger} \text{Tr}_{A \cup \Gamma} [e^{-i\mathcal{H}t} \zeta_{\nu} \otimes \rho^{\Gamma} \otimes \rho^B e^{i\mathcal{H}t}] \right] \\ &= \langle \mathbb{1}^A \otimes \mathbb{1}^{\Gamma} \otimes \zeta_{\mu}^{\dagger}(t) \rangle_{\nu} \end{aligned} \quad (6)$$

where $\langle \cdot \rangle_{\nu} \equiv \text{Tr}[\cdot \zeta_{\nu} \otimes \rho^{\Gamma} \otimes \rho^B]$. Notice that the initial state of the qubit A does not enter the expression of $T_{\mu\nu}(t)$, setting this procedure in the framework of general tomographic approaches.

Let us now consider the time evolution of the quantum state describing the qubit-pair CUB when the total system is initially prepared in the state $\rho^{\text{tot}} =$

$\rho^{\text{CA}} \otimes \rho^{\text{A}} \otimes \rho^{\text{B}}$. By a trivial generalization of the description introduced at the beginning of this section, we write $\rho^{\text{CA}} = g_{\mu\nu}^{\text{CA}} \zeta_{\mu} \otimes \zeta_{\nu}$, and find

$$\rho^{\text{CB}}(t) = \left[g_{\mu\lambda}^{\text{CA}} T_{\nu\lambda}(t) \right] \zeta_{\mu} \otimes \zeta_{\nu} \equiv g_{\mu\nu}^{\text{CB}}(t) \zeta_{\mu} \otimes \zeta_{\nu} . \quad (7)$$

This equation shows that $T_{\mu\nu}(t)$ is the only ingredient needed not only for deriving the dynamics of the qubit B, but also of the qubit pair CUB, providing the pair CUA was prepared separately from the rest of the system, and C is non-interacting [22]. In particular, if C and A are initially prepared in one of the Bell states, say $(|00\rangle + |11\rangle)/\sqrt{2}$, it is $g_{\mu\nu}^{\text{CA}} = \frac{1}{2}\delta_{\mu\nu}$ (similar conditions hold for the other Bell states), i.e.,

$$\rho_{\text{Bell}}^{\text{CA}} = \frac{1}{2} \zeta_{\mu} \otimes \zeta_{\mu} , \quad (8)$$

and hence

$$\rho_{\text{Bell}}^{\text{CB}}(t) = \frac{1}{2} T_{\nu\mu}(t) \zeta_{\mu} \otimes \zeta_{\nu} . \quad (9)$$

The trace-preserving property of the dynamical map, $\text{Tr}[\mathcal{E}_t \zeta_{\mu}] = \text{Tr} \zeta_{\mu}$, together with the specific choice of the basis $\{\zeta_{\mu}\}$, entails $T_{12} + T_{42} = T_{13} + T_{43} = 0$ and $T_{11} + T_{41} = T_{14} + T_{44} = 1$; the Hermiticity of ρ^{B} further implies that $T_{\mu 1} a_{\mu}$ and $T_{\mu 4} a_{\mu}$ are real and $T_{\mu 2} a_{\mu} = T_{\mu 3}^* a_{\mu}^*$. Moreover, from Eq. (6) it clearly follows that symmetry properties of the total Hamiltonian and of the initial state $\rho^{\text{A}} \otimes \rho^{\text{B}}$ may result in constraints for the matrix elements $T_{\mu\nu}$. In particular, when both are symmetric under rotations around the z -axis, it is

$$T_{\mu 2} = T_{2\mu} = T_{22} \delta_{\mu 2} , \quad T_{\mu 3} = T_{3\mu} = T_{33} \delta_{\mu 3} , \quad (10)$$

and only three matrix elements, say T_{11} , T_{22} , and T_{44} , need to be determined.

B. Quality of transfer processes

In order to study the quality of the transfer processes mediated by the spin chain, we specifically consider the entanglement transfer from CUA to CUB, when the former spin pair is initially prepared in a pure state. In this case, the entanglement fidelity, which is a proper measure of the quality of entanglement transmission, reads $\mathcal{F}_{\text{ent}}(t) \equiv \text{Tr}[\rho^{\text{CA}\dagger} \rho^{\text{CB}}(t)]$, which is, via Eq. (7),

$$\mathcal{F}_{\text{ent}}(t) = T_{\mu\nu}(t) (g_{\lambda\mu}^{\text{CA}})^* g_{\lambda\nu}^{\text{CA}} . \quad (11)$$

The entanglement fidelity measures how close the state of CUB at time t is to the initial state of CUA. In particular, if C and A are initially prepared in a Bell state, Eq. (8), it is

$$\mathcal{F}_{\text{ent}}^{\text{Bell}}(t) = \frac{1}{4} T_{\mu\mu}(t) , \quad (12)$$

while the entanglement of the pair CUB is measured by

$$\mathcal{C}_{\text{CB}}^{\text{Bell}}(t) = \frac{1}{2} \mathcal{C}[T_{\nu\mu}(t) \zeta_{\mu} \otimes \zeta_{\nu}] , \quad (13)$$

where $\mathcal{C}[\rho]$ is the concurrence [23] between two qubits in the state ρ . Note that Eqs. (9), (12), and (13) are independent of which Bell state is chosen, since different Bell states are connected to $(|00\rangle + |11\rangle)/\sqrt{2}$ by unitary operations on C, which is isolated.

Another relevant tool for evaluating the quality of the transfer processes is the fidelity of transmission from A to B, which reads $\mathcal{F}_{\text{AB}}(t) \equiv \text{Tr}[\rho^{\text{A}\dagger} \rho^{\text{B}}(t)]$ provided that ρ^{A} is a pure state, i.e., by Eq. (4),

$$\mathcal{F}_{\text{AB}}(t) = b_{\mu}(t) a_{\mu}^* = T_{\mu\nu}(t) a_{\mu}^* a_{\nu} . \quad (14)$$

If A is initially prepared in the state $|\psi_{\theta\varphi}\rangle = \cos\frac{\theta}{2}|0\rangle + e^{i\varphi} \sin\frac{\theta}{2}|1\rangle$, meaning $a_1 = \cos^2\frac{\theta}{2}$, $a_4 = \sin^2\frac{\theta}{2}$, and $a_2 = a_3^* = e^{i\varphi} \sin\frac{\theta}{2} \cos\frac{\theta}{2}$, Eq. (14) can be averaged over all possible initial pure states by integrating over the Bloch sphere, resulting in

$$\overline{\mathcal{F}}_{\text{AB}}(t) = \frac{1}{3} + \frac{1}{6} T_{\mu\mu}(t) , \quad (15)$$

which can be compared with Eq. (12) to obtain the relation [24, 25]

$$\overline{\mathcal{F}}_{\text{AB}}(t) = \frac{1}{3} + \frac{2}{3} \mathcal{F}_{\text{ent}}^{\text{Bell}}(t) . \quad (16)$$

It is worth noticing that a high average fidelity could still allow for states that are poorly (or even not at all) transferred, while the ultimate goal is the transmission of *any* state.

When the setup is such that Eqs. (10) hold, from Eqs. (12) and (13) it follows that

$$\mathcal{F}_{\text{ent}}^{\text{Bell}}(t) = \frac{1}{4} (T_{11} + T_{44} + 2 \text{Re} T_{22}) , \quad (17)$$

$$\mathcal{C}_{\text{CB}}^{\text{Bell}}(t) = \max\{0, |T_{22}| - \sqrt{T_{14}T_{41}}\} . \quad (18)$$

Moreover, if A is prepared in the pure state $|\psi_{\theta\varphi}\rangle$, Eq. (14) explicitly reads

$$\begin{aligned} \mathcal{F}_{\text{AB}}(t) &= T_{11} \cos^4 \frac{\theta}{2} + T_{44} \sin^4 \frac{\theta}{2} \\ &+ [2(1 + \text{Re} T_{22}) - (T_{11} + T_{44})] \sin^2 \frac{\theta}{2} \cos^2 \frac{\theta}{2} , \end{aligned} \quad (19)$$

which shows that $f_0 \equiv T_{11}$ and $f_1 \equiv T_{44}$ are the transmission fidelities of the states $|0\rangle = |\psi_{0\varphi}\rangle$ and $|1\rangle = |\psi_{\pi\varphi}\rangle$, respectively, while $f = \frac{1}{2}(1 + \text{Re} T_{22})$ represents the transmission fidelity of the states $(|0\rangle + e^{i\varphi}|1\rangle)/\sqrt{2} = |\psi_{\frac{\pi}{2}\varphi}\rangle$. The fidelity (19) only depends on $\theta \in [0, \pi]$ and its extrema can be easily determined. To this purpose rewrite Eq. (19) as

$$\mathcal{F}_{\text{AB}}(t) = f + \frac{1}{2}(f_0 - f_1) \cos \theta + \frac{1}{2}(f_0 + f_1 - 2f) \cos^2 \theta ; \quad (20)$$

it follows that $\mathcal{F}_{\text{AB}}(t)$ takes the values f_0 and f_1 at the extrema of the range $\cos \theta \in [-1, 1]$ and can have a minimum

$$f_{\text{m}} = f - \frac{1}{8} \frac{(f_0 - f_1)^2}{f_0 + f_1 - 2f} \quad (21)$$

in between provided that $c_m = \frac{f_1 - f_0}{2(f_1 + f_0 - 2f)} \in (-1, 1)$. Therefore the bounds of $\mathcal{F}_{AB}(t)$ are:

$$\mathcal{F}_{AB}^{\min}(t) = \begin{cases} \min\{f_1, f_0\} & \text{if } |c_m| \geq 1 \\ f_m & \text{if } |c_m| < 1 \end{cases}, \quad (22)$$

$$\mathcal{F}_{AB}^{\max}(t) = \max\{f_1, f_0\}. \quad (23)$$

One can see that if $f_1 = f_0$ the best transmitted states are $|0\rangle$ and $|1\rangle$ which, on the other hand, are the best and the worst transmitted ones (or viceversa) if $|c_m| \geq 1$. This peculiar role of the computational states is obviously a consequence of the assumed symmetry.

III. THE XX MODEL

A. Dynamical evolution

In this section we specifically consider the Hamiltonian (1). The system AUB is prepared in the state $\rho^{\text{tot}} = \rho^A \otimes \rho^\Gamma \otimes \rho^B$ where ρ^Γ is any state invariant under rotations around the z -axis, and $\rho^B = b_1 \zeta_1 + b_4 \zeta_4$: this choice fulfills the requisite of $U(1)$ symmetry of $\rho^\Gamma \otimes \rho^B$ leading to Eq. (10). Referring to the usual Jordan-Wigner transformation, we cast Eq. (1) in the fermionic quadratic form

$$\mathcal{H} = \sum_{i,j} c_i^\dagger \Omega_{ij} c_j = \sum_n \omega_n c_n^\dagger c_n, \quad (24)$$

where $\{c_i, c_i^\dagger\}$ are fermionic operators whose nearest-neighbor interaction is described by a $(N+2) \times (N+2)$ tridiagonal mirror-symmetric matrix

$$\Omega = -\frac{1}{2} \begin{bmatrix} 2h_0 & j_0 & & & & & \\ j_0 & 2h & 1 & & & & \\ & 1 & 2h & 1 & & & \\ & & \ddots & \ddots & \ddots & & \\ & & & 1 & 2h & 1 & \\ & & & & 1 & 2h & j_0 \\ & & & & & j_0 & 2h_0 \end{bmatrix}; \quad (25)$$

an orthogonal transformation $\mathcal{O} = \{\mathcal{O}_{ni}\}$ diagonalizes \mathcal{H} (see Appendix A) in terms of Fermi operators $c_n = \sum_i \mathcal{O}_{ni} c_i$ and c_n^\dagger which annihilate/create excitations of energy ω_n [26, 27]. The trivial time-evolution of the c_n 's entails a time-dependent transformation

$$c_i(t) = \sum_{i=0}^{N+1} U_{ij}(t) c_j, \quad (26)$$

where

$$U_{ij}(t) = \sum_n \mathcal{O}_{ni} \mathcal{O}_{nj} e^{-i\omega_n t}. \quad (27)$$

Reminding that $\zeta_{1,4} = \frac{1}{2}(\mathbb{1} \pm \sigma^z)$, $\zeta_2 = \zeta_3^\dagger = \sigma^+$, and that ζ_μ in Eq. (6) acts on the qubit B, and provided that

Eqs. (10) hold, we find

$$\begin{aligned} T_{11}(t) &= |u(t)|^2 + v(t) \\ T_{44}(t) &= 1 - v(t) \\ T_{22}(t) &= -p \langle \sigma_{N+1}^z \rangle u(t) e^{2i\alpha(t)} \end{aligned} \quad (28)$$

where

$$u(t) = |U_{N+1,0}(t)|, \quad (29)$$

$$\alpha(t) = \arg[U_{N+1,0}(t)] \quad (30)$$

$$v(t) = |U_{N+1,N+1}(t)|^2 \frac{\langle \sigma_{N+1}^z \rangle + 1}{2} + C_{N+1}(t), \quad (31)$$

$$C_i(t) = \sum_{j,j'=1}^N U_{ij}^*(t) U_{ij'}(t) \text{Tr} [\rho^\Gamma c_j^\dagger c_{j'}], \quad (32)$$

with $p = \text{Tr}[P\rho^\Gamma]$, and $P = \exp(i\pi \sum_{i=1}^N c_i^\dagger c_i) \equiv \prod_{i=1}^N (-\sigma_i^z)$ is the chain parity operator, which is a constant of motion. In particular, when ρ^Γ is the ground state of the chain, $p = \text{sign}[\det \Omega]$ [27], where Ω is obtained from Ω by referring only to the chain, i.e., deleting the first and last row and column. In our case, $p = (-1)^{[(N \cos^{-1} h)/\pi]}$, where $[\cdot]$ denotes the integer part, meaning that p equals (-1) to the power of the number of negative energy fermionic eigenmodes of Γ . For $h=0$ it reduces to $p = (-1)^{[N/2]}$.

Once the above expressions are evaluated, the dynamics of B directly follows from the initial state of A via Eq. (4). Similarly, the dynamics of the qubit pair CUB follows from the initial state of the qubit pair CUA, via Eq. (7). Moreover, the time evolution of the magnetization along the chain can be straightforwardly obtained from the formalism described above:

$$\langle \sigma_i^z(t) \rangle = |U_{i0}(t)|^2 \langle \sigma_0^z \rangle + |U_{i,N+1}(t)|^2 \langle \sigma_{N+1}^z \rangle + G_i(t), \quad (33)$$

where $G_i(t) = 2C_i(t) + |U_{N+1,0}|^2 + |U_{N+1,N+1}|^2 - 1$. The r.h.s. of Eq. (33) shows three distinct contributions related with the dynamics of the excitations initially present in A, B, and the chain Γ , respectively. For $h=0$ and N even, $G_i(t)=0$, meaning that $\langle \sigma_i^z(t) \rangle$ are solely determined by two traveling excitations, starting from the edges of the chain. These excitations, because of the single-particle nature of the Hamiltonian, do not scatter, which has great relevance as far as the transport properties of the chain are concerned, as discussed in Section IV. On the other hand, when the chain is initialized in the fully polarized state $\bigotimes_{j=1}^N |\downarrow\rangle$ the contribution $C_i(t)$ vanishes and $G_i(t)$ has the only effect of redefining the range of the magnetization during the dynamics.

B. Fidelities and concurrence

We again consider the system ruled by the Hamiltonian (1) in the setup described above, so that Eqs. (10) hold. Using Eq. (28) we find the entanglement fidelity

and the average transmission fidelity of pure states

$$\mathcal{F}_{\text{ent}}^{\text{Bell}}(t) = \frac{1}{4} + \frac{1}{4}u^2(t) - \frac{1}{2}p \cos \alpha \langle \sigma_{N+1}^z \rangle u(t), \quad (34)$$

$$\overline{\mathcal{F}}_{AB}^{\text{pure}}(t) = \frac{1}{2} + \frac{1}{6}u^2(t) - \frac{1}{3}p \cos \alpha \langle \sigma_{N+1}^z \rangle u(t), \quad (35)$$

as well as the concurrence,

$$\mathcal{C}_{\text{CB}}^{\text{Bell}}(t) = \max \{0, \mathcal{C}_0\}, \quad (36)$$

where

$$\mathcal{C}_0 = |p \langle \sigma_{N+1}^z \rangle| u(t) - \sqrt{v(t)[1 - u^2(t) - v(t)]}. \quad (37)$$

From the above formulas it appears that the choice of the initial state $\rho^\Gamma \otimes \rho^B$ plays an important role [28]: in particular, in order to get the largest concurrence it must be

$$p \langle \sigma_{N+1}^z \rangle = \pm 1, \quad (38)$$

meaning that ρ^Γ is an eigenstate of P and the qubit B is initially in a polarized state, $\rho^B = \zeta_1$ or $\rho^B = \zeta_4$; as for the initial state of the channel, the choices range, for example, from its ground state to a fully polarized state. Such limitation in the choice of the initial state might be overcome by applying a two-qubit encoding and decoding on states ρ^A and ρ^B , respectively [19, 29]. Similarly, for the transmission fidelity the condition

$$-p \langle \sigma_{N+1}^z \rangle \cos \alpha = 1 \quad (39)$$

must hold. Notice that the l.h.s. of Eq. (39) follows from the rotation around the z -axis undergone by the state during the transmission and can be treated by choosing a proper magnetic field [2] or the parity of N , as well as by applying a counter-rotation on the qubit B [28].

The above analysis shows that, once condition (39) is fulfilled the quality of the state and entanglement transfer mainly depends on $u(t)$ and increases with it; the residual dependence on $v(t)$ suggests that the latter quantity need being minimized. In Ref. [28] it has been shown that $v(t)$ is exactly zero provided that both Γ and B are initialized in the fully polarized state. On the other hand, since $U_{ij}(t)$ entering Eqs. (29) and (31) is a unitary matrix, if a certain time t^* exists such that $u(t^*)$ is very close to unity, then $v(t^*)$ must be close to zero, no matter the initialization. This situation is related with the optimal dynamics studied in Ref. [6]: such relation stands on the analytical ground developed in the next Section.

IV. OPTIMAL DYNAMICS

We now have the tools for determining the conditions for a dynamical evolution that corresponds to the best quality of the transmission processes. In Appendix A the algebraic problem of diagonalizing the XX Hamiltonian (24) in the case of nonuniform mirror-symmetric endpoint interactions, Eq. (25) is analytically solved. The eigenvalues of Ω can be written as

$$\omega_k = -h - \cos k, \quad (40)$$

in terms of the pseudo-wavevector k , which takes $N+2$ discrete values k_n in the interval $(0, \pi)$: from Eqs. (A15) and (A16) it follows that these values obey

$$k_n = \frac{\pi n + \varphi_{k_n}}{N+3}, \quad (n = 1, \dots, N+2), \quad (41)$$

with

$$\varphi_k = 2k - 2 \cot^{-1} \left(\frac{\cot k}{\Delta} \right) \in (-\pi, \pi), \quad (42)$$

$$\Delta = \frac{j_0^2}{2 - j_0^2}, \quad (43)$$

where we have set $h_0 = h$. From the above equations it follows that the k 's correspond to the equispaced values $\pi n/(N+3)$, slightly shifted towards $\pi/2$ of a quantity which is smaller than $\pi/(N+3)$, so that their order is preserved: therefore k can be used as an alternative index for n , understanding that it takes the values k_n , as done in Eq. (40). According to the conclusions of the previous section, we focus on the transition amplitude, Eqs. (27) and (29)-(30), which explicitly reads:

$$U_{N+1,0}(t) \equiv u(t)e^{i\alpha(t)} = - \sum_n \rho(k_n) e^{i(\pi n - \omega_{k_n} t)}, \quad (44)$$

where, after Eq. (A21), it is

$$\rho(k) = \frac{1}{N+3} \frac{\Delta(1+\Delta)}{\Delta^2 + \cot^2 k}, \quad (45)$$

and mirror symmetry is exploited according to Eq. (A3): the transition amplitude above is a superposition of phase factors with normalized weights, $\sum_n \rho(k_n) = 1$, entailing $|u(t)| \leq 1$ with equality holding when all phases are equal. The distribution $\rho(k)$ is peaked at $k = k_0 = \pi/2$ and its width is characterized by the parameter Δ , Eq. (43), so that the smaller j_0 the narrower $\rho(k)$.

As $u(t)$ essentially measures the state-transfer quality, the condition for maximizing it at some time t^* , i.e. $u(t^*) \simeq 1$, is that all phases $\pi n - \omega_{k_n} t^*$ almost equal each other. Assume for a moment that the k 's be equispaced values, as in (A8), and that the dispersion relation be linear, $\omega_k = vk$: then Eq. (44) would read

$$u(t) = \left| \sum_n \rho(k_n) e^{i\pi n(1-t/t^*)} \right|, \quad (46)$$

with $t^* = (N+3)/v$, so that $u(t^*) = \sum_n \rho(k_n) = 1$, i.e., all modes give a coherent contribution and entail perfect transfer. On the other hand, in our case ω_k is nonlinear in k , and the k_n are not equally spaced due to the phase shifts (42) entering Eq. (41), so generally the different modes undergo dispersion and lose coherence.

A. Transfer regimes

The dependence of Δ upon j_0 reveals the possibility of identifying different dynamical regimes, characterized by a qualitatively different distribution $\rho(k)$, Eq. (45), and hence, as for the transfer processes, a different behavior of the transition amplitude $u(t)$. For extremely small j_0 the distribution $\rho(k)$ can be so thin that (for even N) only two opposite small eigenvalues come into play, say differing by $\delta\omega$, and perfect transmission will be attained at a large time $t = \pi(\delta\omega)^{-1}$ (for odd N there is a third vanishing eigenvalue at $k = \pi/2$ and still the two identical spacings $\delta\omega$ do matter). This is the Rabi-like regime also mentioned in the Introduction.

A different regime is observed when j_0 is increased: a few more eigenvalues come into play and it may occur, in a seemingly random way, that their spacings be (almost) commensurate with each other, i.e., they can be approximated as fractions with the same denominator K , yielding phase coherence at $t_K = \pi K$. By recording the maximum of $u(t)$ over a fixed large time interval T , as j_0 is varied (see Ref. [3]), a rapid and chaotic variation is observed. This regime is clearly useless for the purpose of quantum communication.

As j_0 further increases, the ballistic regime eventually manifests itself: $\rho(k)$ involves so many modes that commensurability is practically impossible, and a more regular behavior with short transmission time $t^* \sim N$ sets in. The ballistic regime is characterized by relatively large values of $u(t^*, \Delta)$ which is the quantity plotted in Fig. 2, reporting numerical results for increasing chain lengths. It appears that each curve shows a maximum for a particular *optimal* value of $\Delta = \Delta^{\text{opt}}(N)$ or, equivalently, of $j_0 = j_0^{\text{opt}}(N)$: such maxima are remarkably stable for very high N and yield very high transmission quality. In Table I we report some of the optimal values $\Delta^{\text{opt}}(N)$ and $j_0^{\text{opt}}(N)$ for a wide interval of chain lengths. This last ‘ballistic-transfer’ regime is the one we are interested in, since it has two strong advantages: first, the transmission time $t^* \sim N$ is the shortest attainable, and second, the maximum value $u(t^*, \Delta^{\text{opt}})$ of $u(t^*, \Delta)$ is such that one can achieve very good state transfer, e.g., the corresponding transmission fidelity is far beyond the classical threshold, even for very long chains.

The above analysis gives a physical interpretation of what is observed in Fig. 3 of Ref. [3], where the Rabi-like, intermediate and ballistic regimes emerge.

A qualitative picture of the ballistic regime can be obtained by viewing the transition amplitude (44) as a wavepacket with $N+2$ components. It can be evaluated by progressively adding the contributions from symmetric eigenvalues, i.e., for odd N summing between $(N+1)/2 \mp \ell$, for $\ell = 0, 1, \dots, (N+1)/2$. This yields the partial sum $u_\ell(t^*)$ shown in Fig. 3, together with the corresponding frequency and density. One can see that the amplitude increases only over the modes of the linear-frequency zone, i.e. where frequencies are equally spaced, indicating that only those wavepacket components whose

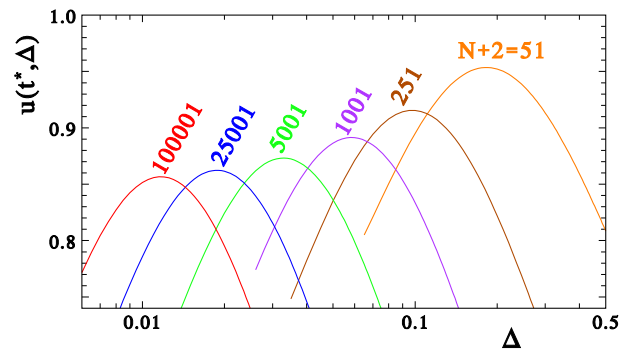


FIG. 2. (color online) Value of $u(t^*, \Delta)$ as a function of Δ , for different wire lengths N . t^* is obtained numerically by maximizing Eq. (44) around $t \simeq N+3$.

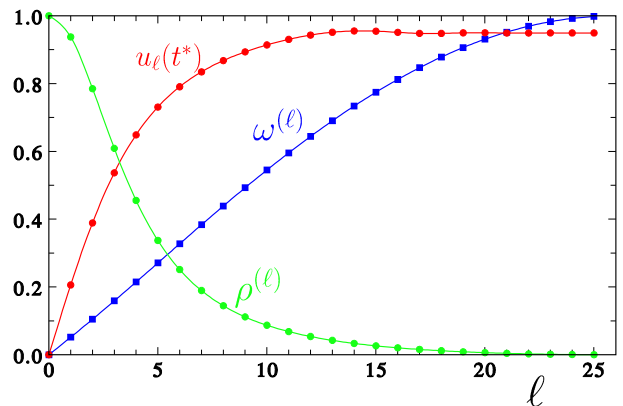


FIG. 3. (color online) Partial sum of the amplitude $u_\ell(t^*)$ vs ℓ for $N+2=51$ and $j_0=0.58$, together with the corresponding frequency and density.

frequency lies in such zone play a role in the transmission process.

B. Ballistic regime and optimal values

From the above reasoning, since the modes contributing to the amplitude lie in a range of size Δ around k_0 , in order to get high-quality transfer processes it is necessary that the corresponding frequencies be almost equally spaced, meaning that ω_{k_n} is approximately linear in n . Actually, ω_k has an inflection point in k_0 : its nonlinearity is of the third order in $k - k_0$ and the modes close to k_0 satisfy the required condition. However, from the phase-shifts (42) a further cubic term arises, which depends on Δ . As Δ varies with j_0 , the latter can be chosen so as to eliminate the cubic terms, yielding a wide interval with almost constant frequency spacing. The latter can be expressed just as the derivative of ω_{k_n} with respect to n , $\partial_n \omega_{k_n} = \sin k \partial_n k$. The last term is evaluated from

$N+2$	25	51	101	251	501	1001	2501	5001	10001	25001	50001	100001	250001	500001
Δ^{opt}	0.245	0.182	0.139	0.098	0.075	0.058	0.042	0.033	0.026	0.019	0.015	0.012	0.009	0.007
j_0^{opt}	0.628	0.556	0.494	0.422	0.374	0.332	0.284	0.252	0.224	0.192	0.171	0.152	0.130	0.116
$u(t^*, \Delta^{\text{opt}})$	0.972	0.953	0.936	0.916	0.902	0.891	0.880	0.873	0.868	0.862	0.859	0.857	0.854	0.853

TABLE I. Optimal values Δ^{opt} and the corresponding j_0^{opt} and $u(t^*, \Delta^{\text{opt}})$ (see text for details), for different N .

Eqs. (41) and (42),

$$\partial_n k = \frac{\pi + \varphi'_k \partial_n k}{N+3} = \frac{\pi}{N+3 - \varphi'_k}, \quad (47)$$

$$\varphi'_k = -2 \frac{1-\Delta}{\Delta} + \frac{2(1-\Delta^2) \cos^2 k}{\Delta[\Delta^2 + (1-\Delta^2) \cos^2 k]}, \quad (48)$$

so that

$$\begin{aligned} \partial_n \omega_{k_n} &= \frac{\pi \sin k}{N+3 - \varphi'_k} \\ &= \frac{\pi}{t^*} \left[1 + \left(2 \frac{1-\Delta^2}{t^* \Delta^3} - \frac{1}{2} \right) \cos^2 k + O(\cos^4 k) \right], \end{aligned} \quad (49)$$

where $t^* = N+3 + 2(1-\Delta)/\Delta$ is the arrival time. It follows that one can minimize the nonlinearity of ω_{k_n} by setting the width to the value Δ_0 satisfying

$$\Delta_0 = \left[\frac{4}{t^*} (1-\Delta_0^2) \right]^{1/3} \xrightarrow{N \gg 1} 2^{2/3} N^{-1/3}, \quad (50)$$

and $j_0 \simeq 2^{5/6} N^{-1/6}$ for large N . Therefore the main mechanism that produces an optimal ballistic transmission is that of varying the endpoint exchange parameter to the value j_0 that ‘linearizes’ the dispersion relation. Actually, if the corresponding $\Delta_0 = \Delta(j_0)$ is such that $\rho(k)$ exceeds the region of linearity, further gain arises by lowering j_0 so as to tighten the relevant modes towards k_0 . However, at the same time ω_{k_n} becomes less linear and the trade-off between these two effects explains why a maximum is observed. This is well apparent in Fig 4, where for different values of Δ the shapes of $\partial_n \omega_k$ can be compared with the excitation density $\rho(k)$: for $\Delta = \Delta_0$ the density still has important wings in the nonlinear zone, so the optimal value Δ^{opt} turns out to be smaller.

The dynamics in the ballistic regime is best illustrated by the time evolution of the magnetization Eq. (33) along the chain, plotted in Fig. 5 when the initial state is $|\uparrow\rangle \otimes |\downarrow \downarrow \cdots \downarrow\rangle \otimes |\uparrow\rangle$. The initial magnetizations at the endpoints generate two traveling wavepackets: for non-optimal couplings ($j_0 = 1$, upper panel) they change their shape and quickly straggle along the chain; for optimal coupling ($j_0 = j_0^{\text{opt}}$, lower panel) they travel with minimal dispersion. This confirms that the coherence is best preserved when the optimal ballistic dynamics is induced: In the next session we show that to such dynamics do in fact correspond high values of the quality estimators for the state and entanglement transfer.

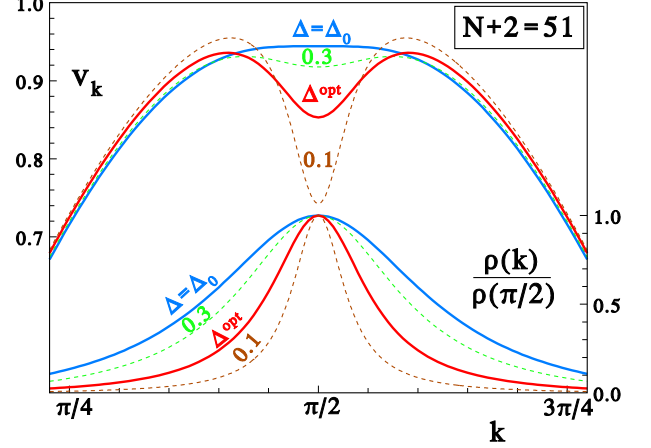


FIG. 4. (color online) ‘Group velocity’ $v_k \equiv [(N+3)/\pi] \partial_n \omega_{k_n}$ and $\rho(k)$ vs k for different values of Δ . The thicker curves correspond to $\Delta_0 = 0.3944$ (50) that gives the flat behavior at k_0 , and to $\Delta^{\text{opt}} \simeq 0.1825$.

V. INFORMATION TRANSMISSION EXPLOITING OPTIMAL DYNAMICS

The requirement Eq. (39), means that the state is not rotated by the dynamics when it arrives on site B, though during the evolution it may undergo a rotation around the z axis. In Ref. [20] it has been shown that $\alpha = -\frac{\pi}{2}(N+1)$ at the transmission time t^* . Therefore, also without applying a counter-rotation on qubit B [28], condition (39) can be fulfilled by choosing $N = 4M \pm 1$ where the sign \pm is given by (38) and thus depends on the initial state of the chain. In the following we assume that conditions (38) and (39) are always satisfied.

Let us consider for the moment that Γ and B are initially in the fully polarized state $|\downarrow \downarrow \cdots \downarrow\rangle \otimes |\downarrow\rangle$. In that case $v(t) \equiv 0$ and the transmission fidelities (34) and (35), as well as the concurrence (36), only depend on, and monotonically increase with, $u(t)$. The best attainable information transfer quality corresponds therefore to the maximum amplitude $u_{\text{opt}} \equiv u(t^*, \Delta^{\text{opt}})$. In Fig. 6 and in Table I we report these values together with the corresponding optimal Δ^{opt} as a function of the chain length N in a logarithmic scale; the inset shows that Δ^{opt} obeys the same power-law behavior predicted in Eq. (50) for Δ_0 . Fig. 6 also shows that for larger and larger N the maximal amplitude u_{opt} does not decrease towards zero, but it rather tends to a constant value of about 0.85, which is surprisingly high, as, e.g., it corresponds to an

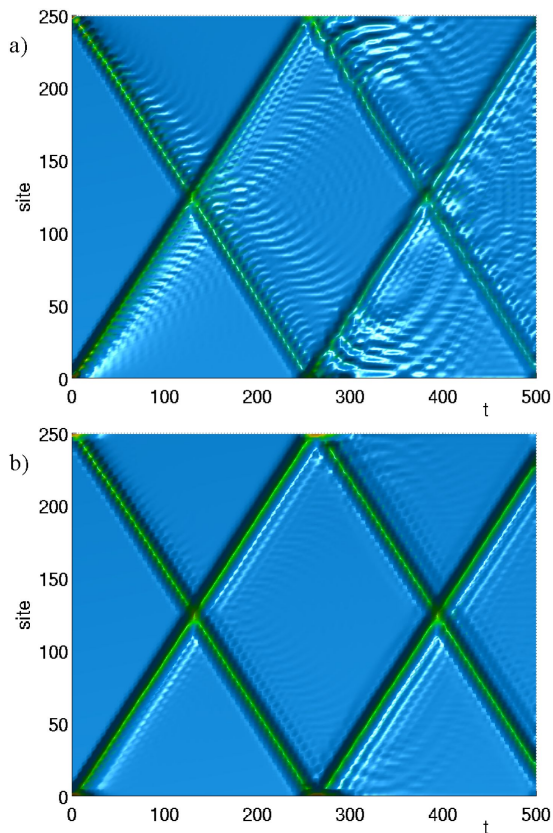


FIG. 5. (color online) Dynamics of the magnetization $\sigma_i^z(t)$ at time t and site i when a) $j_0 = 1$ and b) $j_0 = j_0^{\text{opt}}$. The initial state of the whole system is $|\uparrow\rangle \otimes |\downarrow \downarrow \cdots \downarrow\rangle \otimes |\uparrow\rangle$ and the length of the chain is $N + 2 = 250$.

average fidelity $\overline{\mathcal{F}}_{\text{AB}}(t^*) \gtrsim 0.9$. This is indeed true: We show in Appendix B that in the limit of $N \rightarrow \infty$ the optimized amplitude tends to $u_{\text{opt}} = 0.8469$. Basically, this tells us that it is possible to transmit quantum states with very good quality also over macroscopic distances. From Eq. (B14) we can derive the asymptotic behavior of the optimal coupling

$$j_0^{\text{opt}} \simeq 1.030 N^{-1/6}. \quad (51)$$

In the optimal ballistic case the channel initialization is not crucial, as different initial states satisfying (38) give rise to almost the same dynamics as discussed at the end of subsection III B. In fact, the term $C_{N+1}(t)$ entering Eq. (31) essentially embodies the effect of channel initialization and it is expected to be small at $t = t^*$. This is apparent in Fig. 7, where for $j_0 = j_0^{\text{opt}}$, $C_{N+1}(t^*)$ stays well below 0.1 for N as long as 1000.

The transmitted entanglement, as measured by the concurrence (36), is shown in Fig. 8 as a function of j_0 and t , with the channel initially prepared in its ground state. As expected, the peak of the transmitted concurrence is observed for $j_0 = j_0^{\text{opt}}$; away from j_0^{opt} the quality of transmission falls down because $u(t^*)$ decreases

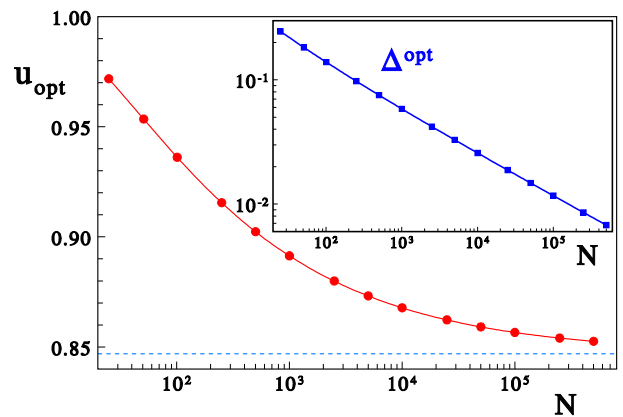


FIG. 6. (color online) Behavior of the maximum attainable amplitude u_{opt} and (inset) of the corresponding optimal value of Δ^{opt} vs logarithm of the chain length N . The horizontal dashed line is the infinite N limit of u_{opt} .

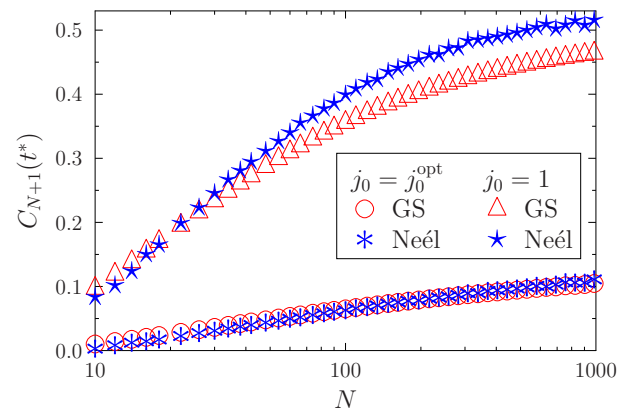


FIG. 7. (color online) $C_{N+1}(t^*)$ for different initial states of the chain (ground state, anti-ferromagnetic Neel state, and series of singlets [28]) when $j_0 = j_0^{\text{opt}}$ and $j_0 = 1$. The results for a series of singlets are numerically indistinguishable from those with the Neel state.

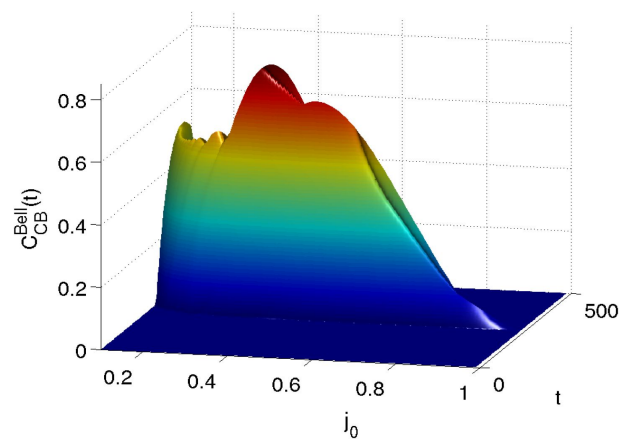


FIG. 8. (color online) Evolution of the concurrence $C_{\text{CB}}^{\text{Bell}}$ vs j_0 and t . The length of the chain is $N + 2 = 250$.

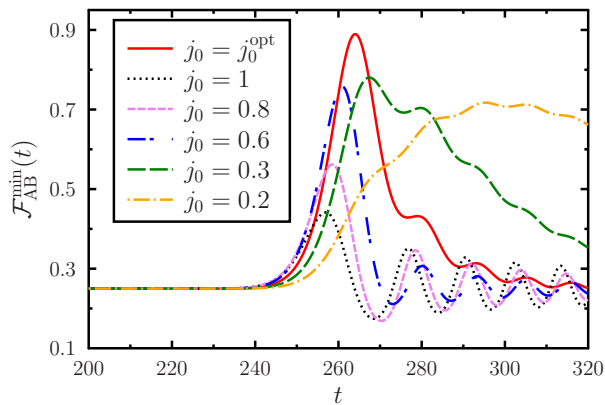


FIG. 9. (color online) Minimum fidelity vs time for different values of j_0 . The length of the chain is $N + 2 = 251$ and $j_0^{\text{opt}} = 0.422$.

and, accordingly, $v(t^*)$ is allowed to increase. In fact, in the non-optimal ballistic case the quality of entanglement transfer does depend on the initial state of the channel [28, 30]; for instance, when $j_0 = 1$ and the chain is initially in its ground state, the contribution of the overlap terms $\text{Tr}[\rho^\Gamma c_j^\dagger c_{j'}]$ in Eq. (32) is not quenched by the dynamical prefactors, and higher values of $C_{N+1}(t^*)$ (see Fig. 7) inhibit the transmission of entanglement even if $u(t^*) \neq 0$.

The effect of the optimization of j_0 is clearly evident in the time behavior of the minimum fidelity, Eq. (22), reported in Fig. 9. The peak of $\mathcal{F}_{\text{AB}}^{\text{min}}(t)$ for j_0^{opt} occurs at the arrival time $N+3+s$ with a time delay s that agrees with the asymptotic value $s \simeq 2.29 N^{1/3}$ derived in Appendix B. The ‘reading time’, i.e., the time interval during which the qubit B keeps being in the transferred quantum state, is $t_{\text{R}} \simeq \Delta^{-1}$, as the same figure also shows; note that, in the optimal case, t_{R} increases with N according to the asymptotic behavior $t_{\text{R}} \simeq 1.89 N^{1/3}$.

VI. CONCLUSIONS

In this paper we have shown that high-quality quantum state and entanglement transfer between two qubits A and B is obtained through a uniform XX channel of arbitrary length N by a proper choice of the interaction j_0 between the channel and the qubits. The value of such interaction is found to control the transfer regime of the channel, which varies, as j_0 increases, from the Rabi-like one, characterized by very long transmission time, to an intermediate regime, which turns useless for the purpose of quantum communication, and finally becomes ballistic for j_0 of the order of the intrachannel interaction.

In order to get coherent transfer in the ballistic regime, it is desirable that the k -density of the traveling wavepacket generated by Alice’s initialized qubit A be narrow and concentrated in the linear zone of the dis-

person relation, i.e., with equispaced frequencies. As the parameter j_0 controls both the width of the k -density and the spacings of the frequencies entering the dynamics, one can therefore improve the transmission quality up to a best trade-off arising for an optimal value $j_{\text{opt}}(N)$ which for large N behaves as $j_{\text{opt}}(N) \simeq 1.03 N^{-1/6}$. Remarkably, we have found that for such a choice the quantum-state-transfer quality indicators are very high and, indeed, have a lower bound for $N \rightarrow \infty$ that still allows to efficiently perform quantum-information tasks: e.g., the average fidelity of state transmission is larger than 90%.

The ballistic regime ensures fast transmission on a time scale of the order of N , at variance with the Rabi-like regime, and in the optimal case the reading time increases as $N^{1/3}$. It is also to be noted that, if experimental settings constrain to a given value j_0^{exp} , yet one can optimize the chain length in such a way that $j_0^{\text{exp}} = j_0^{\text{opt}}(N)$. The only requirement on the initial state of the receiving qubit B and the spin bus is to possess $U(1)$ symmetry, a condition that can be fulfilled by several configurations concerning the spin bus, ranging from the fully polarized state to the highly-entangled ground state. If a large magnetic field can be switched on during the initialization procedure (in order to fully polarize the channel), and switched off as soon as the transmission starts, then, from our analytical treatment it emerges that temperature is not a major issue as far as the dynamical evolution of the channel is concerned, though low temperatures are obviously necessary to protect the qubits from phase and amplitude damping due to the solid-state environment. To judge if the proposed scheme identifies a reasonable experimental framework, let us estimate the magnitude of the involved physical quantities. Consider a solid-state implementation with lattice spacing of about 10 Å and intrachain exchange $J \simeq 10^2$ K. A quantum state will then be transferred with fidelity 90% along a channel of length 1 cm ($N \simeq 10^7$) using $j_0 \simeq 1.03 N^{-1/6}$ $J \simeq 7.0$ K, with transmission time $t = N \hbar / (k_{\text{B}} J) \simeq 0.75 \mu\text{s}$ and reading time $t_{\text{R}} \simeq 1.9 N^{1/3} \hbar / (k_{\text{B}} J) \simeq 0.03$ ns.

ACKNOWLEDGMENTS

We acknowledge the financial support of the Italian Ministry of University in the framework of the 2008 PRIN program (contract N. 2008PARRTS 003). LB and PV gratefully thank Dr. A. Bayat and Prof. S. Bose for useful discussions, and TJGA thanks ISC-CNR for the kind hospitality.

Appendix A: Quasi-uniform tridiagonal matrices

The matrix Ω , Eq. (25), can be written as $\Omega = -h - \frac{1}{2}\mathcal{M}$ where

$$\mathcal{M}(x, y) = \begin{bmatrix} x & y & & & & & & & \\ y & 0 & 1 & & & & & & \\ & & 1 & 0 & 1 & & & & \\ & & & \ddots & \ddots & \ddots & & & \\ & & & & & 1 & 0 & 1 & \\ & & & & & & & 1 & 0 & y \\ & & & & & & & & y & x \end{bmatrix} \quad (\text{A1})$$

is a square tridiagonal matrix of dimension $M = N + 2$, and $x = 2(h_0 - h)$ and $y = j_0$. This real symmetric matrix is diagonalized by an orthogonal matrix $O(x, y)$,

$$\sum_{i,j=1}^M \mathcal{O}_{ki} \mathcal{M}_{ij} \mathcal{O}_{k'j} = \lambda_k \delta_{kk'} , \quad (\text{A2})$$

and it is known that (i) if $y \neq 0$ the eigenvalues are nondegenerate [31], (ii) the eigenvectors corresponding to the eigenvalues ordered in descending order are alternately symmetric and skew symmetric [32], i.e.,

$$\mathcal{O}_{ki} = \pm \mathcal{O}_{k, M+1-i} . \quad (\text{A3})$$

The eigenvalues are the roots of the associated characteristic polynomial

$$\chi_M(\lambda; x, y) \equiv \det[\lambda - \mathcal{M}(x, y)] . \quad (\text{A4})$$

In the fully uniform case the characteristic polynomial is $\eta_M(\lambda) \equiv \chi_M(\lambda; 0, 1)$ and one easily obtains the recursion relation

$$\eta_M = \lambda \eta_{M-1} - \eta_{M-2} , \quad (\text{A5})$$

that can be solved in terms of Chebyshev polynomials of the second kind,

$$\eta_M = \frac{\sin(M+1)k}{\sin k} , \quad (\text{A6})$$

where

$$\lambda \equiv 2 \cos k , \quad (\text{A7})$$

so the eigenvalues of $\mathcal{M}(0, 1)$ correspond to M discrete values of k ,

$$k = \frac{\pi n}{M+1} \quad [n = 1, \dots, M] ; \quad (\text{A8})$$

the corresponding eigenvectors are

$$\mathcal{O}_{ki}(0, 1) = \sqrt{\frac{2}{M+1}} \sin ki . \quad (\text{A9})$$

The general determinant (A4) can be expressed in terms of the η_M 's by expanding it in the first and then in the last column,

$$\chi_M = (\lambda^2 - 2x\lambda + x^2) \eta_{M-2} - 2y^2(\lambda - x) \eta_{M-3} + y^4 \eta_{M-4} , \quad (\text{A10})$$

and using Eq. (A5) one can eliminate the explicit appearances of λ ,

$$\chi_M = \eta_M - 2x \eta_{M-1} + x^2 \eta_{M-2} + (1-y^2)[2 \eta_{M-2} - 2x \eta_{M-3} + (1-y^2) \eta_{M-4}] \quad (\text{A11})$$

By rewriting Eq. (A6) as $\sin k \eta_M = \text{Im} [e^{i(M+1)k}]$ and defining

$$z^2 \equiv 1 - y^2 , \quad z_k^2 \equiv z^2 e^{-2ik} , \quad x_k \equiv x e^{-ik} , \quad (\text{A12})$$

$$u_k \equiv 1 - x_k + z_k^2 = e^{-ik} \{ [(2-y^2) \cos k - x] + i y^2 \sin k \} , \quad (\text{A13})$$

Eq. (A11) takes the form

$$\sin k \chi_M(k) = \text{Im} \{ e^{i(M+1)k} u_k^2 \} . \quad (\text{A14})$$

The secular equation $\text{Im} \{ e^{i(M+1)k} u_k^2 \} = 0$ entails that when k corresponds to an eigenvalue the quantity in braces is real and equal to either $\pm |u_k|^2$; by Eq. (A13) it turns into $\sin [(M+1)k - \varphi_k] = 0$, with the phase shift

$$\varphi_k = 2k - 2 \tan^{-1} \frac{y^2 \sin k}{(2-y^2) \cos k - x} , \quad (\text{A15})$$

so the M eigenvalues correspond to

$$k_n = \frac{\pi n + \varphi_{k_n}}{M+1} , \quad (n = 1, \dots, M) . \quad (\text{A16})$$

We are interested in the squared components of the first column of the diagonalizing matrix \mathcal{O}_{ki} , which can be expressed as [31]

$$\mathcal{O}_{k1}^2 = \frac{\xi_{M-1}(\lambda_k)}{\partial_\lambda \chi_M(\lambda_k)} = - \frac{2 \sin k \xi_{M-1}(k)}{\partial_k \chi_M(k)} , \quad (\text{A17})$$

where k assumes the values (A16) and $\xi_{M-1}(\lambda; x, y)$ is the characteristic polynomial associated to the first minor matrix \mathcal{M}_{11} that, expanded in the last column and using Eq. (A5), reads

$$\begin{aligned} \xi_{M-1} &\equiv \det[\lambda - \mathcal{M}_{11}(x, y)] \\ &= (\lambda - x) \eta_{M-2} - y^2 \eta_{M-3} \\ &= \eta_{M-1} - x \eta_{M-2} + (1-y^2) \eta_{M-3} . \end{aligned} \quad (\text{A18})$$

Then the numerator of Eq. (A17) is

$$\sin k \xi_{M-1} = \text{Im} \{ e^{iMk} u_k \} , \quad (\text{A19})$$

while from Eq. (A14) one has

$$\begin{aligned} \sin k \partial_k \chi_M(k) &= (M+1) \text{Re} \{ e^{i(M+1)k} u_k^2 \} \\ &\quad + 2 \text{Im} \{ e^{i(M+1)k} u_k u'_k \} , \end{aligned} \quad (\text{A20})$$

where the argument of Re is real indeed; retaining only the dominant term for $M \gg 1$ Eq. (A17) becomes

$$\mathcal{O}_{k_1}^2 = \frac{2}{M+1} \frac{y^2 \sin^2 k}{[(2-y^2) \cos k - x]^2 + y^4 \sin^2 k}. \quad (\text{A21})$$

For $x = 0$ the above expression is in agreement with Ref. [3]. In the most common case $x < 2-y^2$ the maximum k_0 of $\mathcal{O}_{k_1}^2$ is located at

$$\cos k_0 = \frac{x}{2-y^2}, \quad (\text{A22})$$

so that switching x on the maximum shifts from $\pi/2$ to

$$k_0 = \frac{\pi}{2} - \sin^{-1} \frac{x}{2-y^2}; \quad (\text{A23})$$

the ‘eigenvalue’ corresponding to the maximum is

$$\lambda_0 = 2 \cos k_0 = \frac{2x}{2-y^2} \quad (\text{A24})$$

so that for $y \sim 1$, the maximum shifts the ‘energy’ linearly with x . Expanding $\mathcal{O}_{k_1}^2$ around the maximum, the leading behavior is found to be a Lorentzian,

$$\mathcal{O}_{k_1}^2 \simeq \frac{2}{M+1} \frac{y^2}{y^4 + [(2-y^2)^2 - x^2](k - k_0)^2}, \quad (\text{A25})$$

whose width (HWHM) is given by

$$\Delta \simeq \frac{y^2}{\sqrt{(2-y^2)^2 - x^2}}. \quad (\text{A26})$$

When x and y are small, $k_0 \simeq (\pi-x)/2$ and $\Delta \simeq y^2/2$, so x rules the position of the peak, while y determines its width.

Appendix B: large- N limit of the amplitude

The transition amplitude, Eq. (44), in the case of odd $N = 2M-1$ reads

$$u(t) = \frac{\Delta(1+\Delta)}{N+3} \sum_{m=-M}^M \frac{e^{i(\pi m - t \sin q_m)}}{\Delta^2 + \tan^2 q_m}, \quad (\text{B1})$$

where the summation has been made symmetric through the change of variable $q = \pi/2 - k$. The shift equation (41) turns into

$$\pi m = (N+3) q_m + \pi \varphi_{q_m}, \quad (\text{B2})$$

with

$$\pi \varphi_q = 2 \left(\tan^{-1} \frac{\tan q}{\Delta} - q \right). \quad (\text{B3})$$

In the limit $N \rightarrow \infty$ one can write the sum as an integral setting

$$\frac{1}{N+3} \sum_m \rightarrow \int \frac{dq}{\pi} \left(1 + \frac{\pi \varphi'_q}{N+3} \right) \rightarrow \int \frac{dq}{\pi}. \quad (\text{B4})$$

As we deal within the region of the optimal value of $\Delta \sim N^{-1/3} \rightarrow 0$, we have

$$u_\infty(t) = \lim_{N \rightarrow \infty} \Delta \int_{-\pi/2}^{\pi/2} \frac{dq}{\pi} \frac{e^{i[(N+3)q + \pi \varphi_q - t \sin q]}}{\Delta^2 + \tan^2 q}. \quad (\text{B5})$$

Writing the arrival time as $t = N+3 + s$, where s is the arrival delay, one has then

$$u_\infty(t) = \lim_{t \rightarrow \infty} \Delta \int_{-\pi/2}^{\pi/2} \frac{dq}{\pi} \frac{e^{i[t(q - \sin q) - sq + \pi \varphi_q]}}{\Delta^2 + \tan^2 q} \quad (\text{B6})$$

The relevant q 's are of the order of $\Delta \sim N^{-1/3} \rightarrow 0$, so we change to $q = \Delta x$, with x of the order of 1; keeping the leading terms for $\Delta \rightarrow 0$,

$$t(q - \sin q) \rightarrow \frac{t \Delta^3}{6} x^3, \quad (\text{B7})$$

$$\pi \varphi_q \rightarrow 2 \tan^{-1} x, \quad (\text{B8})$$

$$\frac{\Delta dq}{\Delta^2 + \tan^2 q} \rightarrow \frac{dx}{1+x^2}, \quad (\text{B9})$$

and defining the rescaled counterparts of the arrival time $t \simeq N$ and of the delay $s \sim N^{1/3}$,

$$\tau \equiv \frac{\Delta^3}{6} t, \quad \sigma \equiv \Delta s; \quad (\text{B10})$$

the final asymptotic expression results

$$u_\infty(\tau, \sigma) = \int_{-\infty}^{\infty} \frac{dx}{\pi} \frac{e^{i(\tau x^3 - \sigma x + 2 \tan^{-1} x)}}{1+x^2}, \quad (\text{B11})$$

that can also be rewritten in the form of a simple summation of phases by introducing the variable $z = \tan^{-1} x$,

$$u_\infty(\tau, \sigma) = \frac{2}{\pi} \int_0^{\pi/2} dz \cos(\tau \tan^3 z - \sigma \tan z + 2z). \quad (\text{B12})$$

As in the finite- N case, one has to maximize $u_\infty(\tau, \sigma)$ by finding the optimal values of σ and τ . For $\tau = 0$ it is easy to evaluate Eq. (B11) analytically,

$$u_\infty(0, \sigma) = 2 e^{-\sigma} \sigma; \quad (\text{B13})$$

it is maximal for $\sigma = 1$, giving $u(0, 1) = 2e^{-1} \simeq 0.736$, to be regarded as a lower bound to the overall maximum of $u_\infty(\tau, \sigma)$. The overall maximization has been performed numerically using Eq. (B12). It turns out that the maximum corresponds to $\sigma = 1.2152$ and $\tau = 0.02483$, and amounts to $u_\infty(0.02483, 1.2152) = 0.84690$, in agreement with the behavior shown in Fig. 6. The resulting scaling, from Eq. (B10), tells that asymptotically

$$\Delta \simeq 0.530 N^{-1/3}, \quad s \simeq 2.29 N^{1/3}. \quad (\text{B14})$$

-
- [1] S. Bose, *Contemp. Phys.* **48**, 13 (2007).
- [2] S. Bose, *Phys. Rev. Lett.* **91**, 207901 (2003).
- [3] A. Wójcik *et al.*, *Phys. Rev. A* **72**, 034303 (2005).
- [4] T. J. G. Apollaro and F. Plastina, *Phys. Rev. A* **74**, 062316 (2006).
- [5] L. Campos Venuti, S. M. Giampaolo, F. Illuminati, and P. Zanardi, *Phys. Rev. A* **76**, 052328 (2007).
- [6] L. Bianchi *et al.*, *Phys. Rev. A* **82**, 052321 (2010).
- [7] C. Ramanathan, P. Cappellaro, L. Viola, and D. G. Cory, arXiv:1102.3400 (2011).
- [8] A. Zwick and O. Osenda, *J. Phys. A* **44**, 105302 (2011).
- [9] M. Christandl *et al.*, *Phys. Rev. A* **71**, 032312 (2005).
- [10] P. Karbach and J. Stolze, *Phys. Rev. A* **72**, 030301 (2005).
- [11] C. Di Franco, M. Paternostro, and M. S. Kim, *Phys. Rev. Lett.* **101**, 230502 (2008).
- [12] A. Zwick, G. A. Álvarez, J. Stolze, and O. Osenda, arXiv:1105.0071 (2011).
- [13] M. L. Hu and H. L. Lian, *Eur. Phys. J. D* **55**, 711 (2009).
- [14] E. B. Fel'dman, E. I. Kuznetsova, and A. I. Zenchuk, *Phys. Rev. A* **82**, 022332 (2010).
- [15] T. J. Osborne and N. Linden, *Phys. Rev. A* **69**, 052315 (2004).
- [16] H. Yadsan-Appléby and T. J. Osborne, arXiv:1102.2427 (2011).
- [17] M.-H. Yung and S. Bose *Phys. Rev. A* **71**, 032310 (2005).
- [18] G. Gualdi, V. Kostak, I. Marzoli, and P. Tombesi, *Phys. Rev. A* **78**, 022325 (2008).
- [19] N. Y. Yao *et al.*, *Phys. Rev. Lett.* **106**, 040505 (2011).
- [20] L. Bianchi, A. Bayat, P. Verrucchi, and S. Bose, *Phys. Rev. Lett.* **106**, 140501 (2011).
- [21] M. A. Nielsen and I. L. Chuang, *Quantum information and computation* (Cambridge University Press, Cambridge, 2000).
- [22] C. Di Franco, M. Paternostro, G. M. Palma, and M. S. Kim, *Phys. Rev. A* **76**, 042316 (2007).
- [23] W. K. Wootters, *Phys. Rev. Lett.* **80**, 2245 (1998).
- [24] M. A. Nielsen, *Phys. Lett. A* **303**, 249 (2002).
- [25] M. Horodecki, P. Horodecki and R. Horodecki, *Phys. Rev. A* **60**, 1888 (1999).
- [26] E. Lieb, T. Schultz, and D. Mattis, *Ann. Phys.* **16**, 407 (1961).
- [27] M. Cozzini, P. Giorda, and P. Zanardi, *Phys. Rev. B* **75**, 014439 (2007).
- [28] A. Bayat, L. Bianchi, S. Bose, and P. Verrucchi, arXiv:1104.0718 (2011).
- [29] M. Markiewicz and M. Wieśniak, *Phys. Rev. A* **79**, 054304 (2009).
- [30] A. Bayat and S. Bose, *Phys. Rev. A* **81**, 012304 (2010).
- [31] B. N. Parlett, *The Symmetric Eigenvalue Problem* (SIAM, Philadelphia, 1998).
- [32] A. Cantoni and P. Butler, *Linear Algebra Appl.* **13**, 275 (1976).